CSIRO PUBLISHING

International Journal of Wildland Fire
https://doi.org/10.1071/WF21062

Do you CBI what I see? The relationship between the Composite Burn Index and quantitative field measures of burn severity varies across gradients of forest structure

Saba J. Saberi[A,B], *Michelle C. Agne*[A] *and Brian J. Harvey*[A]

[A]School of Environmental and Forest Sciences, University of Washington, Seattle, WA 98195, USA.
[B]Corresponding author. Email: sjsaberi@uw.edu

Abstract. Burn severity in forests is commonly assessed in the field with visual ordinal estimates such as the Composite Burn Index (CBI). However, how CBI (a composite of several individual field measures) relates to independent quantitative measures of burn severity (e.g. fire-caused tree mortality, surface charring) has not been widely tested. Here, we use field data from 315 plots in 14 fires in the north-western USA to ask: (1) how CBI relates to eight independent field measures of burn severity; and (2) how these relationships vary across gradients of pre-fire forest structure. Overall, CBI corresponded well with most independent field measures, but some measures of extreme burn severity (e.g. deep charring on trees and snags) were not captured by CBI. Additionally, some measures of canopy burn severity corresponded to lower CBI values in forests with larger average tree size (diameter and height) – potentially from decoupling of surface and canopy fire effects in stands with larger, fire-resistant trees. Our findings suggest continued broad utility of CBI, while highlighting how the correspondence of aggregate plot-level CBI to different measures of burn severity can vary with forest conditions. We also suggest considerations for broadening CBI to account for more extreme levels of burn severity.

Keywords: Cascade Mountains, conifer forests, deep char, fire ecology, fire effects, north-western USA, Rocky Mountains, tree mortality.

Received 12 May 2021, accepted 24 November 2021, published online 11 January 2022

Introduction

Fire shapes terrestrial ecosystems worldwide (Bowman *et al.* 2009), highlighting the importance of monitoring fire effects over space and time (Eidenshink *et al.* 2007; Picotte *et al.* 2020). One important dimension of fire activity is burn severity – the magnitude of ecological change caused by fire – which is often characterised as fire-caused vegetation mortality, charring, or combustion of biomass (Keeley 2009). Burn severity has been a major focus of fire ecology since the early 2000s (Keeley 2009; Morgan *et al.* 2014) and is useful for characterising contemporary fire regimes (e.g. Miller *et al.* 2009; Dillon *et al.* 2011; Cansler and McKenzie 2014; Harvey *et al.* 2016). As climate warming and increasing fire activity drive changes in fire regimes worldwide (Abatzoglou and Williams 2016; Westerling 2016; Johnstone *et al.* 2016), consistently measuring burn severity across space and time is critical for understanding fire-driven shifts in ecosystems.

The Composite Burn Index (CBI; Key and Benson 2006) was initially developed in 1996 (following analysis of 1994 wildfires in Glacier National Park) as a standardised field measure of burn severity for calibrating satellite-derived indices of fire-caused change. The most commonly used satellite indices are based on the Normalized Burn Ratio (NBR), which detects fire effects based on differences in the near-infrared band (NIR) and the short-wave infrared band (SWIR) – two spectral bands that correspond to fire-caused vegetation changes (Knipling 1970). CBI is a unitless index of burn severity recorded in a 30-m circular plot (to match Landsat satellite pixel resolution) where field technicians visually reconstruct pre-fire conditions and estimate the fire-caused change. CBI is calculated from semi-quantitative ocular estimation of fire-caused change in up to five strata, which are each assigned a number ranging between zero (unburned) and three (high severity, or high levels of fire-caused change) (Key and Benson 2006). CBI is useful in that it is fairly quick to implement in the field and corresponds well with field measures based on plant injury, fuel consumption and tree mortality (Miller *et al.* 2009). As such, CBI is the most widely used field protocol for quantifying burn severity (Dragozi *et al.* 2016) and has aided in calibrating maps of satellite indices of burn severity to an on-the-ground index over wide regions (Allen and Sorbel 2008; Miller *et al.* 2009; Soverel *et al.* 2010; Cansler and McKenzie 2012, Parks *et al.* 2019).

Despite widespread use, how consistently CBI captures different dimensions of burn severity has not been tested widely. The CBI of a field plot is commonly computed by collapsing ocular estimates from different components (e.g. tree mortality, scorch height, soil charring) within and among strata into one number for the whole plot. This process can obscure many dimensions of burn severity and may miss important differences among components of burn severity (e.g. differences between tree mortality and soil charring; Morgan *et al.* 2014). Variants of CBI have been developed to assign weights to each stratum or component by their fractional cover (Geo CBI in the sense of De Santis and Chuvieco 2009 or Weighted CBI as used by Soverel *et al.* 2011), but the original CBI remains widely used. CBI data come from ocular estimates and require extrapolation of pre- to post-fire change, and therefore user or analyst subjectivity could affect accuracy or precision. Among experienced forestry professionals, there can be up to 16% disagreement in ocular estimations of canopy cover (Korhonen *et al.* 2006; Miller *et al.* 2009). In addition, while CBI was developed to be an index of relative change that is applicable across forest types, it is not known if CBI performs similarly across gradients of forest structure (e.g. in stands with larger trees vs. smaller trees).

Other field protocols have been developed that directly measure and quantify independent components of burn severity, using plot configurations similar to CBI (e.g. Hudak *et al.* 2007; Miller and Thode 2007; Harvey *et al.* 2014*a*, 2019; Andrus *et al.* 2016; Whitman *et al.* 2018). For example, proportion surface char, proportion bole char (Harvey *et al.* 2013, 2014*b* referred to this as 'bole scorch') and proportion needle scorch can be directly measured on individual trees within a plot. Similarly, measurements of tree populations and fire-caused mortality within a census of all trees in a plot can provide direct measures of the proportion of trees or tree basal area killed by fire (Harvey *et al.* 2019, Furniss *et al.* 2020). Quantitative protocols for directly measuring burn severity, while more time-intensive than CBI, can provide detailed information about independent measures of burn severity and can connect specific fire effects to processes (Morgan *et al.* 2014). For example, deep charring on wood is the thermally altered remnants of incompletely combusted vegetation, which occurs when fire intensity is very high and/or when the woody material is already dead and fuel moisture content is high (Baldock and Smernik 2002; Donato *et al.* 2009). Quantifying the presence and abundance of deep char can provide insights into fire intensity and/or sustained smouldering combustion (Donato *et al.* 2009; Bird *et al.* 2015). Further, directly measured variables are less prone to subjectivity by the recorder than are ocular estimates (Korhonen *et al.* 2006). However, to our knowledge, few comprehensive comparisons between CBI and multiple quantitative field measures of burn severity collected in the same plot exist (but see Whitman *et al.* 2018) – likely because independent measurements of burn severity and CBI are rarely co-located (Morgan *et al.* 2014).

In this study, we use multiple field measures of burn severity (CBI and eight independent quantitative measures) in 315 field plots in recently burned forests across the north-western USA to address two research questions. (1) How does CBI relate to eight independent quantitative field measures of burn severity? (2) How does the relationship between CBI and independent quantitative field measures differ across gradients of forest structure?

Methods

Study area

The study area covers an elevation gradient from 400 to 2200 m and moisture gradient from continental to maritime (approx. 50–250 cm annual precipitation) (PRISM Climate Group, available at https://prism.oregonstate.edu/normals/), containing forests from the west side of the Cascade Mountains to the US Northern Rockies (Table 1 and Fig. 1). Forested areas of the north-western USA are characterised by a wide spectrum of historical fire regimes ranging from frequent low-severity fires (every ~5 years with little overstorey tree mortality) to infrequent high-severity fires (occurring every 2–5 centuries with near-complete overstorey tree mortality) (Agee 1996; Baker 2009). In general, fire frequency is inversely related to fire severity; shorter intervals between fires correspond to lower severity and vice versa (Agee 1996). Forests are conifer-dominated, with a variety of species possessing different fire-adapted traits. Thick-barked species (e.g. *Pinus ponderosa* (ponderosa pine), *Larix occidentalis* (western larch)) that can survive frequent, low-severity fires occur at relatively low-elevation, warm and dry locations, while thin-barked species that are adapted to colonise or invade from seed (e.g. *Pinus contorta* (lodgepole pine) and *Abies lasiocarpa* (subalpine fir)) following infrequent, high-severity fire occur at relatively high-elevation, cool and moist locations (Agee 1996; Baker 2009).

Table 1. Descriptive statistics of physical setting and pre-fire stand structure variables across all 315 plots

DBH, diameter at breast height; QMD, quadratic mean diameter

Variable	Min–max	Mean	Median
Physical setting			
Latitude (decimal degrees)	43.8–47.4	45.4	44.4
Longitude (decimal degrees)	–122.6 to –110.7	–117.9	–120.9
Elevation (m)	408–2227	1480	1447
Slope (degrees)	0.3–37.4	13.6	12.8
Heat load (MJ cm^{-2} $year^{-1}$)	0.06–1.42	0.50	0.27
Pre-fire stand structure			
Basal area (m^2 ha^{-1})	0.4–144.0	28.4	20.9
Stand density (stems ha^{-1})	111–133 800	2715	1422
Large trees only (>10 cm DBH)	67–22 554	1015	623
QMD (all trees, cm)	0.2–79.8	19.1	15.6
QMD (all trees live at fire)	0.5–74.3	21.9	19.2
Maximum tree height (m)	1.4–68.3	18.0	16.8
Mean tree height (m)[A]	2.2–49.3	16.8	15.6
Pre-fire live canopy cover (as prop.)	0.48–0.99	0.69	0.66

[A]Of 20 tallest trees in plot

Field data collection

We sampled fires across gradients of burn severity, fire regimes and forest zones from 14 fires in nine National Forests and two National Parks across the north-western USA (Supplementary Table S1). During the summers of 2017 and 2018, we collected post-fire burn severity data in the field from forests that had burned 1 year before sampling (2016 and 2017, respectively). Unburned plots were also sampled in each fire, and were located either within the fire perimeter in unburned stands or outside the fire perimeter in analogous forest conditions. Unburned plots were located an average of 359 m outside fire perimeters; however, three unburned plots in one fire were located in analogous stands 12 km from the fire perimeter, as an active fire burning during fieldwork limited access to immediate proximity. Plots were separated by a minimum

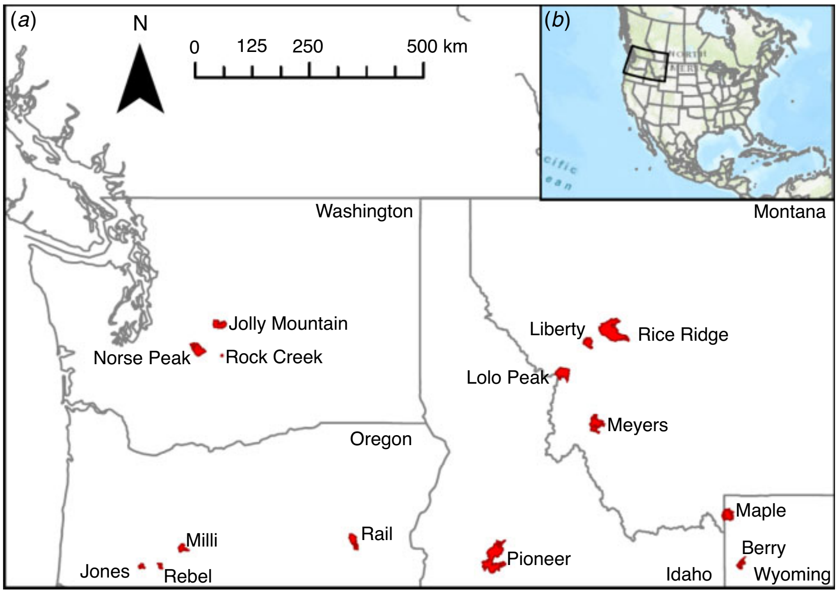

Fig. 1. Map of study area with each fire (in red) sampled in this study.

distance of 400 m to mitigate potential pseudo-replication from spatially correlated burn severity (Harvey *et al.* 2013) and were located a minimum of 100 m from roads or trails. Within each fire, plots were evenly distributed among four categories of observed fire effects corresponding to likely fire behaviour: unburned (no fire effects observed); light surface fire (forest floor vegetation burned, but little charring/scorching high on tree boles); severe surface fire (most forest floor vegetation burned and moderate to high levels of overstorey tree mortality); and crown fire (canopy trees charred and near or actual 100% tree mortality).

Each plot was a 30-m diameter circle divided into four quadrants using two 30-m transect tapes oriented in the four cardinal directions. Within each plot, we followed the CBI protocol (Key and Benson 2006) by recording visually estimated fire effects across five forest strata: (1) substrate; (2) herbs, low shrubs and trees <1 m tall; (3) tall shrubs and trees 1 to >5 m tall; (4) sub-canopy trees; (5) upper canopy trees in a 30-m diameter circular plot. We assigned index values to the nearest 0.1 between 0.0 and 3.0 to each stratum, with 0 indicating no fire effects (unburned) and 3.0 indicating maximum burn severity (e.g. mortality of all vegetation). The index values for each stratum were averaged to obtain a single plot-level CBI estimate. For consistency in CBI measurements across plots, field personnel conducting CBI assessments were consistent across all plots, and the protocol was first calibrated with the fire effects team at Grand Teton National Park. In addition, CBI was collected in each plot before quantitative measures of burn severity were recorded so as to not bias CBI estimates from prior knowledge of measured burn severity in a plot.

Field measurements

Immediately after recording CBI estimates in each plot, we collected field data to calculate eight quantitative measures of burn severity, five from the canopy and three from the forest floor (Tables 2, 3, 4, Fig. 2). Canopy measures of burn severity included: proportion of tree mortality by basal area and by number of trees, proportion change in live canopy cover, an ordinal index of tree live and dead needle retention (Table 2), the proportion of charred tree bole circumference (considered a canopy measure because it is a strong predictor of tree mortality; Harvey *et al.* 2013, 2014*a*, 2014*b*, 2019; Andrus *et al.* 2016), char height, an ordinal index of deep char (Table 3) and proportion surface char.

In each plot, all trees in the 30-m circular plot were measured for diameter at breast height (dbh, or 1.37 m), identified to species, and assigned as live, dead or killed by fire, or dead and killed before fire. Next, canopy cover was measured using a densiometer and tallying the number of squares with live vegetation, dead vegetation, or open sky in all four cardinal directions at 3-, 9-, 21- and 27-m marks along both transects (24 total points in each plot). All other independent tree-related measures (dead needle index, bole char, char height and deep char) were recorded for the 20 tallest trees per plot (the five tallest trees within each of the four quadrants of the circular plot). These 20 tallest trees were assigned a needle index value from 1 to 7 (Table 2). To record bole char, we visually estimated the proportion of bole circumference charred by fire on each of the 20 trees. Tree height was measured to the nearest 0.1 m on each of the 20 trees using a laser rangefinder or avalanche probe for shorter trees, and char height was measured with the laser rangefinder at the highest point of char on the tree bole. Lastly, values for the deep char index were recorded on each of the 20 trees via ocular estimation (Table 3). The percentage of charred surface cover was measured by tallying the surface char (i.e. any charred soil, rock, litter, vegetation every 10 cm along each of the cardinal direction transects from 0 to 12 m and 18 to 30 m, avoiding plot centre where foot traffic during plot installation could have disturbed the forest floor).

Independent metric calculations

Field data were calculated into eight independent metrics of burn severity reported as proportions (continuous values between 0 and 1, including 0 and 1), with each plot assigned a mean value for each variable. For fire-caused change, logical minimum values are 0 (no change) and maximum values are 1.0 (100%), and thus 0–1 (or 0–100%) were set as bounds that values could not exceed. Several metrics required reconstructing pre-fire values to calculate change, whereas others were direct measures of post-fire attributes and did not require reconstructing pre-fire values. The latter condition was especially true when the pre-fire condition could be safely assumed to be zero (e.g. no pre-fire surface char on the forest floor).

Fire-caused tree mortality (basal area and number of trees) and canopy cover change required reconstructions of pre-fire values. To calculate proportion tree mortality by number of trees and by basal area, the number of trees and total basal area that were killed by fire were divided by the number of trees and total basal area live at the time of fire, respectively. Fire-caused change in live canopy cover at the plot level was calculated by subtracting the measured post-fire live canopy cover from modelled pre-fire live canopy cover, and dividing by the modelled pre-fire live canopy cover. Pre-fire live canopy cover was modelled for each plot using reconstructed pre-fire live basal area and piecewise linear beta (β) regression models built from analogous data in unburned plots where we had measurements of live canopy cover and live basal area (Supplementary Fig. S1, Tables S2, S3). This approach was chosen as an alternative to modelling pre-fire canopy cover using allometric relationships used in simulation models (e.g. Forest Vegetation Simulator, Crookston and Dixon 2005) that have been applied in other systems (Miller *et al.* 2009). We opted for this approach because we had locally relevant data from unburned plots to build our own plot-level models. In the few cases (approx. 10% of the burned plots) where the model predicted an increase in live canopy cover from pre- to post-fire, values of canopy over change were manually set to zero since a post-fire increase in live canopy cover is unlikely over the period between the fire and our field measurements. Not allowing the responses to exceed zero and one was a requisite of our modelling structure (see data analysis below) and the few instances where the modelled change in live canopy cover indicated an increase were likely an artefact of the uncertainty in the model, as opposed to real changes in canopy cover.

The remaining metrics did not require calculating pre-fire values as they were all assumed to be zero pre-fire. For each measured metric of dead needle index, char height, bole char and deep charring that was recorded for the 20 randomly selected dominant canopy trees, the value was converted to a proportion of maximum for each tree, and averaged across the 20 trees per plot. For example, char height was converted to proportion by dividing char height by the total tree height; a maximum char height of 15 m on a tree that was 20 m tall would receive a score of 0.75 for char height. Surface char was converted to a proportion by dividing the number of 'hits' of surface char on the ground cover survey by the total number of points surveyed

Table 2. Descriptions of each possible value for the dead needle index

Index value	Description
1	Live tree, brown needles along 0–5% of total tree height
2	Live tree, brown needles along 5–50% of total tree height
3	Live tree, brown needles along >50% total tree height
4	Dead tree, retains >50% of needles
5	Dead tree, retains 5–50% of needles
6	Dead tree, retains <5% of needles
7	Dead tree, retains <5% of needle-bearing branches

Table 3. Descriptions of each possible value for the deep char index

Index value	Description
0	No deep char present
1	Deep char present around base of bole, not into crown
2	Deep char present into crown of tree

Table 4. Description of Composite Burn Index (CBI) and all independent field measures of burn severity, and the range, median and mean of their values across all 315 plots

Variable name	Variable description	Range	Median	Mean
CBI	Average CBI value per plot, converted to proportion from the 0–3 scale	0–1	0.47	0.43
Change in live canopy cover	Average proportion change in live canopy cover per plot. Proportion of pre-fire canopy in burned plots was modelled using the relationship between plot basal area and proportion of live canopy in from unburned plots	0–1	0.56	0.51
Dead needle	Average needle index value per plot, averaged from 20 randomly selected trees alive at time of fire, converted to proportion from 0–7 scale	0–1	0.44	0.44
Killed BA	Proportion of average tree basal area alive at time of fire and killed by fire per plot	0–1	0.31	0.44
Killed trees	Proportion of average number of trees alive at time of fire killed by fire per plot	0–1	0.63	0.53
Char height	Average proportion of total tree height charred from 20 randomly selected dominant canopy trees alive at time of fire	0–1	0.23	0.38
Bole char	Average proportion of visible char on 20 randomly selected dominant canopy trees alive at time of fire	0–1	0.99	0.66
Deep char	Average deep char index value on 20 randomly selected dominant canopy trees alive at time of fire, converted to proportion from 0–2 scale	0–1	0	0.03
Surface char	Average proportion of plot containing charred material on surface, taken from 480 points every 10 cm apart along main plot axis (N–S, E–W)	0–1	0.16	0.28

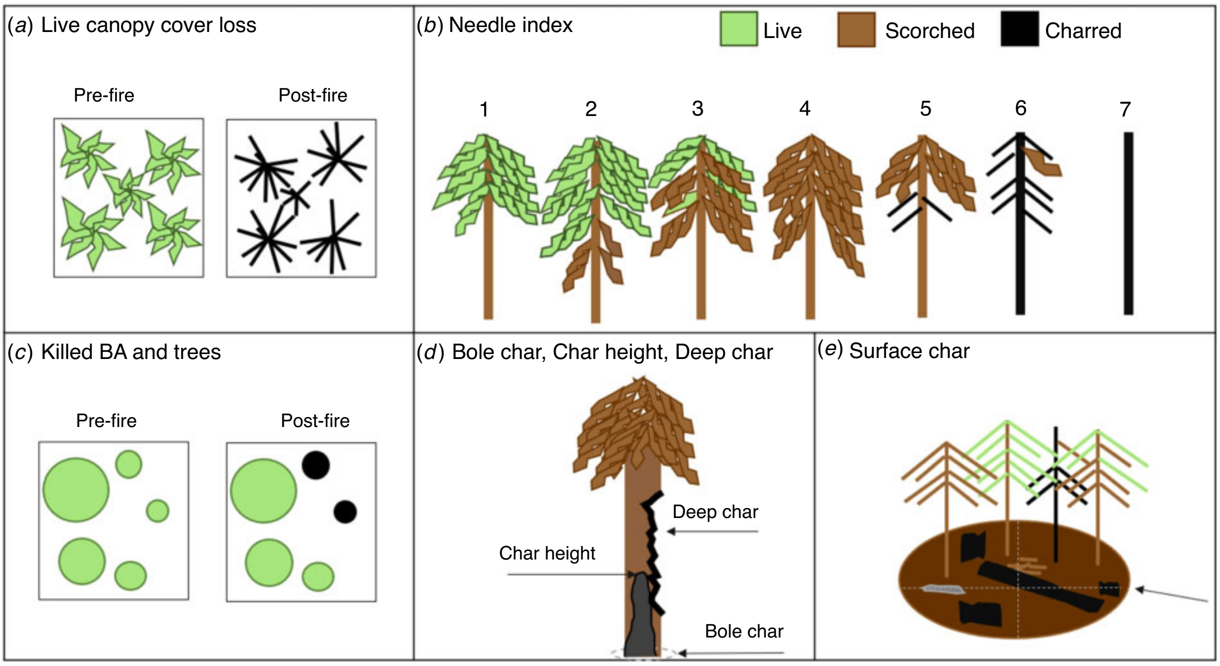

Fig. 2. Schematic representing the eight independent field measures: (*a*) shows how 100% canopy cover loss comes from a fully live canopy transitioning to a fully dead canopy; (*b*) shows each of the seven index values; (*c*) represents killed basal area and trees with an aerial view of boles; (*d*) represents deep char, char height and bole char on a single tree; and (*e*) shows how surface char is measured along two transect lines.

(480 points). For example, a plot with 360 hits of charred material on the forest floor would receive a score of 0.75 for surface char.

To characterise pre-fire stand structure in each plot, we also calculated the following five stand structure variables from field measurements: stand density (stems ha^{-1}), basal area (m^2 ha^{-1}), quadratic mean diameter (cm), mean tree height (m), pre-fire live canopy cover (proportion, modelled as previously described). Stand density, basal area and mean quadratic diameter were derived from independent measurements taken from every tree in the plot (complete population survey). Mean tree height was derived from the heights of the 20 tallest trees in the plot and therefore represents the mean height of canopy-dominant trees.

Data analysis

For ease of comparison among variables, each field measure that was not originally measured as a proportion was converted from its native scale and units to a continuous proportion ranging from 0 (unburned) to 1 (maximum possible burn severity value). Indices were capped between 0 and 1 because values outside these bounds (e.g. a char height exceeding tree height) are impossible. To test how well CBI corresponds to each quantitative measure of burn severity (Q1), we created zero/one inflated beta (ZOIB) regression models (Ospina and Ferrari 2012) with the quantitative field measure as the response variable and CBI as the predictor variable. We fitted General Additive Models for Location Scale and Shape (GAMLSS) and specified ZOIB distributions to allow for 0, 1 and continuous proportions between 0 and 1 as values for the response variable using the 'gamlss' package in R version 3.4.3. (Rigby and Stasinopoulos 2005; R Core Team 2017). In the ZOIB framework, three parameters are used in the distribution: *mu*, *nu* and *tau* (Ospina and Ferrari 2012). *Mu* represents the mean of the beta distribution when the response is between 0 and 1, exclusive. *Nu* and *tau* represent the probability that the response will be either 0 or 1, and the relationship is as follows:

$$\frac{nu}{1 + nu + tau} = \text{probability of zeros}$$

$$\frac{tau}{1 + nu + tau} = \text{probability of ones}$$

Model uncertainty was quantified using 1000 parametric bootstrap iterations. For each iteration, we simulated data from the original model, fit a new model to the simulated data, and then used the new model to predict each response variable across a range of CBI values between 0 and 3. The 2.5% quantile, mean, and upper 97.5% quantile of the bootstrap predictions were plotted to construct a 95% confidence interval around the mean of the predicted response values.

We evaluated model fit for each of the eight models using the Area Under Receiver Operating Characteristic curves (AUC) over a sequence of proportion thresholds (0.05, 0.275, 0.5, 0.725 and 0.95) for the continuous field measure of burn severity. We also calculated average AUC values across all five thresholds for each of the models (Supplementary Table S6). AUC values were calculated by dichotomising the field response proportions into zeroes and ones for each classification threshold. AUC values below 0.5 indicate poor model fit or capacity to distinguish presence and absence (Pearce and Ferrier 2000). To understand relationships among burn severity metrics, we also compared the pairwise relationships among each of the field measurements using Spearman's rank correlation coefficients.

To test how relationships between CBI and each independent measure of burn severity vary across a gradient of forest stand structure variables (Q2), we built regression models with CBI as the dependent variable, each of the eight field metrics as the respective independent variable, and each of the five stand structure variables as the secondary covariate, or interaction term (model equation: CBI = independent field metric × stand structure variable). In each model, an interaction term tested for an effect of each stand structure variable on the relationship between CBI and each independent measure of burn severity. We tested whether the slopes and intercepts of these models differed when we fixed the value of the stand structure covariate at its 5th, 50th and 95th percentile values using the same bootstrapping technique used for Q1. Analyses for Q2 used the same model framework (ZOIB regressions) and model fit analysis (AUCs for five thresholds) as analyses for Q1. To test for significant effects of interaction terms (and therefore effects of stand structure on the relationship between each independent field measure of burn severity and CBI) for Q2, we considered $P \leq 0.10$ as suggestive evidence, $P \leq 0.05$ as moderate evidence and $P \leq 0.01$ as strong evidence. We use these three cut-offs to mitigate the exclusion of potentially meaningful ecological relationships when analysing inherently noisy observational field data (Ramsey and Schafer 2012).

Results

Independent field measures and CBI

CBI was consistently and positively related to most (seven out of eight) independent measures of burn severity (overall AUC values ≥ 0.86, Fig. 3, Supplementary Tables S5, S6). In general, CBI performed better as a predictor of independent measures of canopy burn severity (Fig. 3*a*–*j*) than independent measures of surface burn severity (Fig. 3*k*–*p*). There was a general trend of consistently high performance (AUC > 0.90) of CBI across the gradient of burn severity percentiles (Fig. 3*b*, *f*, *h*, *p*), with slight-to-modest declines in performance of CBI at upper percentiles (75th and 95th) of burn severity (Fig. 3*d*, *j*, *l*). The two steepest declines of performance for CBI at high levels of burn severity were for the dead needle index (Fig. 3*d*) and char height (Fig. 3*l*). Most independent measures of burn severity (including CBI) were highly correlated with each other ($r \geq 0.80$, Fig. 3).

The relationship between CBI and deep char was an exception to the generally high correspondence between CBI and independent field measures (Fig. 3, Supplementary Table S6). CBI was positively related to deep char (Fig. 3*m*), but to a much weaker degree overall (overall AUC = 0.86 vs ≥ 0.95 for other measures) than were the other independent field measures. The relationship between CBI and deep char also varied in the trend over the gradient of burn severity. AUC increased in the upper percentiles (75th and 95th), contrary to the relationship between CBI and other variables (Fig. 3*n*). Among pairwise correlations between variables, deep char was the least correlated ($r = 0.40$ to 0.54) with other measures or CBI (Fig. 4). The absence of strong evidence that deep char could be reliably modelled from CBI ($P > 0.01$ for *mu*, $P < 0.001$ for *nu* and $P > 0.10$ for *tau* parameters of model) resulted in deep char being not analysed for the second research question.

Independent field measures and CBI across forest structure gradients

Overall, stand structure had a greater effect on the relationship between measures of canopy burn severity and CBI than it did on the relationship between surface burn severity and CBI. In general, for stands with taller and larger trees (greater pre-fire live canopy cover, tree height, basal area and quadratic mean diameter (QMD)), a given CBI value (e.g. 2.0) corresponded to lower values of canopy burn severity than in stands with shorter and smaller trees (Fig. 5*b*1–*b*4 vs *g*). Pre-fire stand density affected fewer relationships between CBI and independent burn severity measures (Fig. 5*a*5–*g*5), but when effects were present, they were generally opposite to those for other stand structure variables (e.g. basal area, QMD).

Relationships between measures of surface burn severity and CBI were less affected by stand structure than were measures of canopy burn severity (Fig. 5). The relationship between char height and CBI was affected by pre-fire stand structure in the same direction, though in lower magnitude than measures of canopy burn severity (i.e. stands with taller and larger diameter trees had lower canopy burn severity for a given value of CBI, Fig. 5). The relationship between bole char and CBI was opposite, in that stands with shorter and smaller diameter trees had lower canopy burn severity for a given value of CBI (Fig. 5).

Discussion

Understanding how CBI relates to independent measures of burn severity across gradients of forest stand structure is important, as CBI is among the most widely used metrics in fire ecology. Our findings suggest that CBI captures many independent components of burn severity across a range of burn severities and forest types throughout a temperate fire-prone forested region. Most independent field measures of burn severity (except for deep char) correspond consistently with CBI, with some variability in the relationships between CBI and each independent measure. In addition, because the relationships between CBI and independent field measures vary by forest structure attributes, understanding such effects can help with interpreting burn severity when CBI is the only information available. Finally, we suggest that recording additional measurements such as deep char to augment CBI can provide important information about sustained smouldering combustion and the consumption of legacy trees (Donato *et al.* 2009) – a dimension of burn severity that is not currently characterised fully by CBI.

Independent field measures of burn severity and their relationship with CBI

Our findings of the individual relationships between CBI and independent measures of burn severity help to inform the utility and potential limits of CBI for inferring different dimensions of fire effects. The consistent correspondence between CBI and canopy measures of burn severity has important implications for the use of CBI as an indicator of burn severity on the live tree population. Our results support findings of a strong relationship

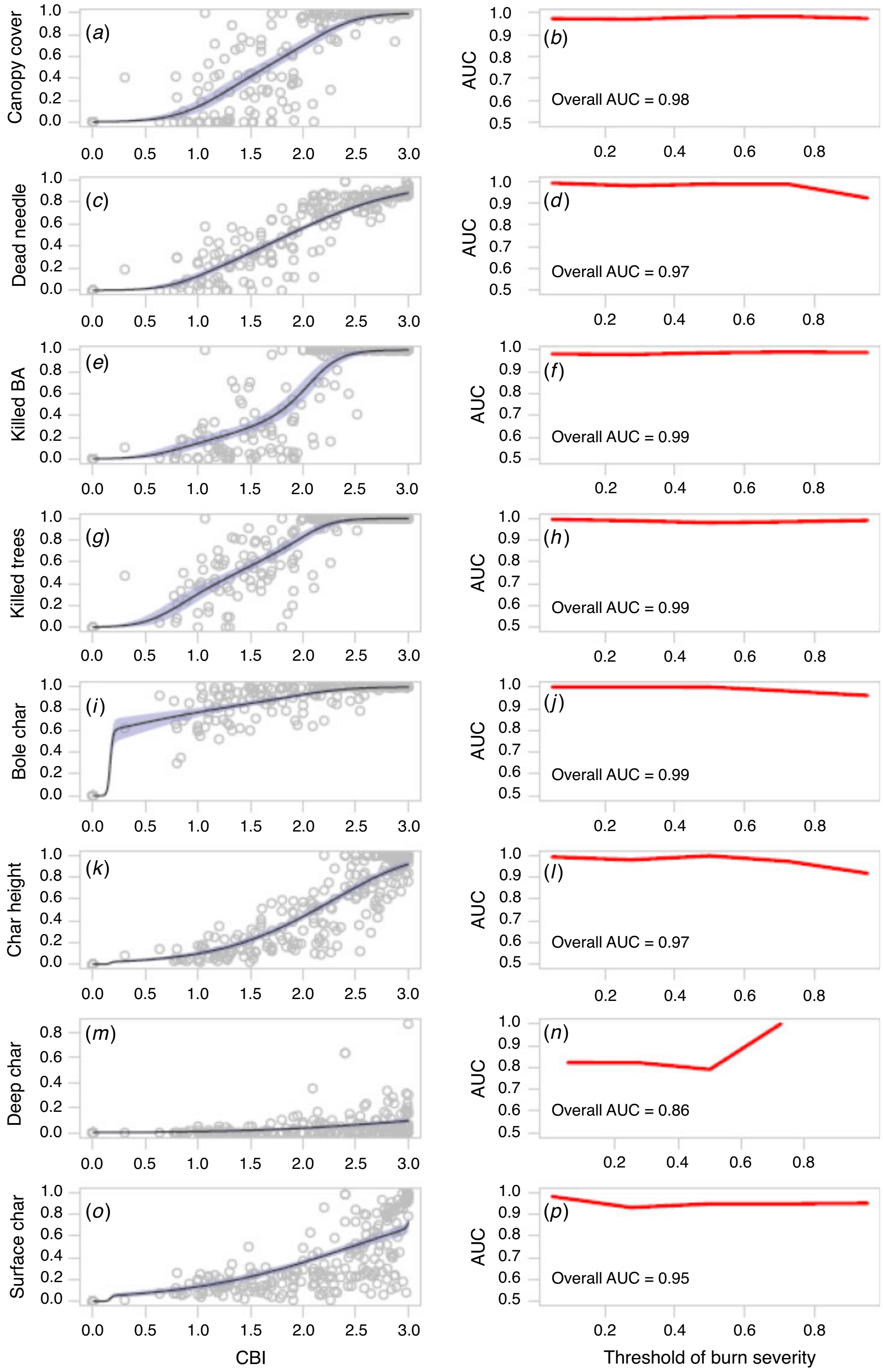

Fig. 3. Zero/one inflated beta regression models for each of the eight independent burn severity metrics with CBI (Composite Burn Index) as the predictor variable. In the first column (panels *a*, *c*, *e*, *g*, *i*, *k*, *m*, *o*), the black line shows model prediction values. The blue polygon around the line shows 95% confidence around mean predicted values from bootstrapping. Gray dots are the raw data points from the 315 sampled plots. The second column (panels *b*, *d*, *f*, *h*, *j*, *l*, *n*, *p*) contain AUC (area under the curve) values for each of the eight regression models across five thresholds of burn severity (which were created as dichotomisation thresholds to produce ROC (receiver operating characteristic) curves). Overall AUC values represent overall average across five thresholds. Thresholds that are the *x*-axis on the right column are derived from the *y*-axis (independent burn severity metric) on the left panels.

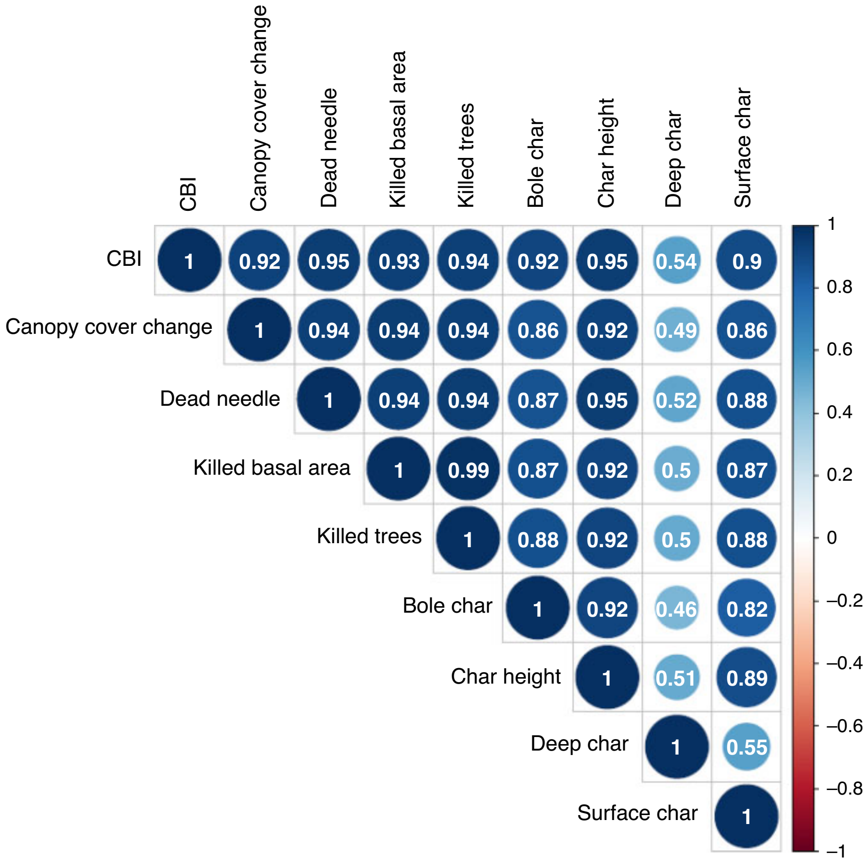

Fig. 4. Correlation matrix for nine burn severity metrics. Larger, darker circles indicate a greater value for Spearman's correlation coefficient. Blue corresponds to a positive correlation and red to a negative correlation.

between CBI and canopy burn severity reported for boreal forests (Whitman *et al.* 2018) and suggest that CBI is consistently related to canopy burn severity across a broad range of conifer forests. This correspondence between CBI and canopy burn severity is important for being able to characterise the effect of fire on post-fire vegetation trajectories. Canopy burn severity can dictate the legacies (remaining live trees as a seed source), given the relationship between canopy burn severity and post-fire tree regeneration (e.g. Harvey *et al.* 2014*b*). In addition, high canopy burn severity can allow more light to reach the understorey, affecting competitive outcomes for understorey vegetation (Brodie *et al.* 2021).

In contrast, our finding that CBI did not correspond well to deep char suggests that CBI may be not fully representing other dimensions of burn severity such as the effect of fire on snags and coarse woody debris and sustained smouldering combustion (Donato *et al.* 2009). This finding has key implications for the use of CBI to infer immediate and post-fire carbon dynamics, which are an understudied dimension of fire effects (Stenzel *et al.* 2019). The lack of strong correspondence between CBI and deep char is likely because the CBI protocol accounts for deep char found on wood on the forest floor, and a CBI of 3.0 can occur with the current CBI protocol even if there is no presence of deep char. However, our field measures included deep char on standing snags and live tree boles. As such, CBI may miss some important dimensions of deep char, such as not capturing the effects of fire on branch and outer wood or bark consumption on snags (Talucci and Krawchuk 2019). Thus, while CBI relates to most independent fire effects within a plot, collecting additional information on deep char – especially on snags – can provide additional key information on important effects across vertical strata.

Our findings that CBI relates to some field measures more poorly at the high end of burn severity has implications for tracking potentially greater levels of burn severity as fire activity increases. Weaker relationships between CBI and independent measures (particularly char height, bole char and the needle index) as burn severity increased suggests that CBI is a better predictor of independent metrics at lower burn severity levels. At the low end (e.g. an unburned plot), the strong relationship between CBI and independent measures of burn severity is a result of both values being bound by zero, creating a region of the data where all points will have perfect correspondence. However, CBI can only go to a maximum value of 3, but a CBI of 3 does not necessarily capture the full range of high severity recorded by independent measures in plots (Morgan *et al.* 2014). For example, a stand with 100% vegetation mortality but snags mostly still intact with little to no deep char can receive a CBI of 3.0, but so can a stand with 100% vegetation mortality and all snags and/or coarse woody debris deeply charred or consumed

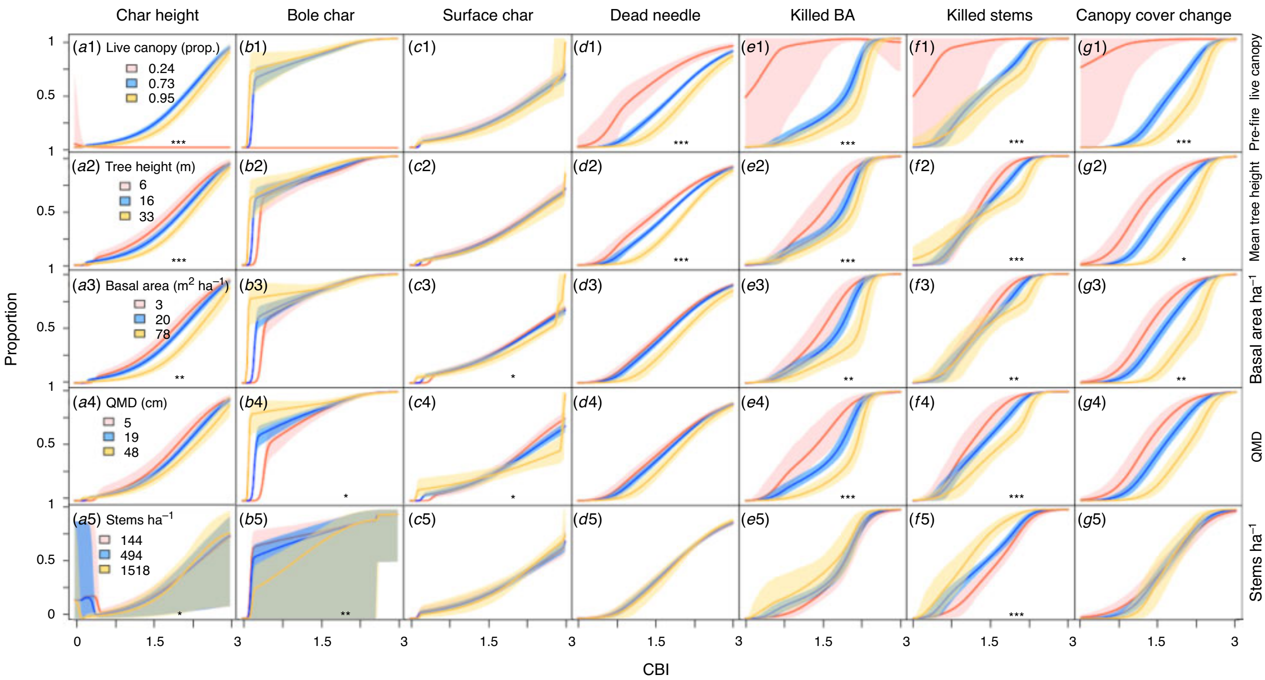

Fig. 5. Zero/one inflated beta regression models for each of the eight independent burn severity metrics with CBI as the predictor variable and each of the five forest stand structure variables as the secondary covariate. The red, blue and yellow lines show the model prediction values when the secondary covariate is fixed at its respective 5th, 50th and 95th quantile values. The asterisks represent the levels of significance on parameters of the interaction term, with one asterisk indicating that at least one parameter in the model has a *P* value <0.1, two indicating that at least one parameter in the model has a *P* value <0.05, and three indicating that at least one parameter has a *P* value <0.01.

(e.g. 'crown fire plus'; Turner *et al.* 2019). In this example, these two stands are equal in fire-caused vegetation mortality but are qualitatively different in other measures of burn severity. This context of burn severity greater than the scale of CBI, with high amounts of deep char produced on logs and snags, is common when fire follows soon after another disturbance such as a beetle outbreak (e.g. Harvey *et al.* 2014*a*; Talucci and Krawchuk 2019) or a prior fire (e.g. Donato *et al.* 2009; Turner *et al.* 2019). In sum, as the current maximum of CBI at 3.0 can include burn severity where little to no deep charring is occurring in a stand, this may mean that increased levels of burn severity are not being captured by CBI and additional information could detect greater degrees of burn severity either with an amended CBI or with ancillary measures.

Differences in relationships between CBI and independent field measures across forest structure gradients

Our finding that the relationship between CBI and independent field measures varies by pre-fire stand structure has implications for the use of CBI as a standardised indicator of burn severity across forest gradients. For example, in forests with taller, larger-diameter trees, there is a greater potential for a decoupling of surface and canopy fire effects. All else equal, larger-diameter and taller trees are generally more fire-resistant (Hood *et al.* 2008; Pausas 2015) and have tree crowns that are physically separated from (i.e. higher above) the forest floor. In our study, the plots with the greatest QMD and tree height were also the plots with the greatest abundance of ponderosa pine and Douglas-fir – two species with high fire resistance for larger individuals (Harvey *et al.* 2013; Dunn and Bailey 2016; Johnston *et al.* 2019; Stevens *et al.* 2020). In such plots, field-based CBI values consistently overestimated canopy mortality, as surface burn severity could be greater (i.e. a higher CBI value) without translating to severe effects on fire-resistant trees. For example, there were some plots where only ~15% of basal area (BA) was killed, but the CBI value was 2.25 (75% of the total CBI scale) or greater because of severe surface burn severity. Conversely, shorter and smaller-diameter trees are generally less fire-resistant, and experience effects more similar to the forest floor vegetation. As such, we found generally similar effects between the surface and canopy severity and more consistent correspondence between CBI and independent measures of burn severity in plots with smaller and shorter trees. Collectively, our findings suggest that using an aggregated value of CBI (often the only available information to users) without information on the forest stand structure can lead to an overprediction of canopy burn severity in cases where large, fire-resistant trees are present.

Suggested augmentation to collecting CBI data

Our study highlights that CBI captures many dimensions of independent measures of burn severity, and that some additional data collection could fill a gap for dimensions of burn severity that CBI does not include. Specifically, in its current form, CBI does not fully capture some components at the extreme high end of burn severity, such as deep charring (or complete combustion) of boles of standing trees and snags, which are of high ecological importance (Donato *et al.* 2009; Turner *et al.*

2019; Talucci and Krawchuk 2019). Given the widespread adoption and high utility of CBI over many decades, it may be a practical solution to include ancillary data on dimensions of burn severity such as deep charring. Such information could be rapidly assessed while continuing to use the current CBI protocol, without a substantive added cost of additional sampling effort, as our findings suggest that most other dimensions of burn severity are captured quite well by CBI. Alternatively, as fire activity changes in many regions worldwide (Pausas and Keeley 2021) and more 'extreme' burn severity is recorded (Turner *et al.* 2019), there may be important opportunities to update CBI so that the maximum end of the scale (currently 3.0) includes more severe fire effects as they are observed.

Management implications

Recent developments in mapping burn severity have moved from mapping burn severity using satellite indices (e.g. the differenced NBR; Miller *et al.* 2009) towards mapping CBI as an index of on-the-ground burn severity (Parks *et al.* 2019). The relationships we show between CBI and independent fire effects can further these developments by converting maps of CBI into maps of independent field measures (e.g. tree basal area loss or surface char) – providing a crosswalk between CBI and individual measures of burn severity. However, testing of the uncertainty in relationships at multiple levels (e.g. field measures and satellite data) warrants further study, as a wide range of fire effects for some measures can result from a single CBI value, particularly at the higher end of CBI. There are few burn severity studies that explicitly incorporate uncertainty into severity maps (Harvey *et al.* 2019; Furniss *et al.* 2020), and they suggest that there is a considerable degree of uncertainty in predictions used in burn severity mapping. With uncertainty quantified, maps can show the predicted value of burn severity measures, as well as the range of likely outcomes for different metrics at each location (Harvey *et al.* 2019; Furniss *et al.* 2020). Given the widespread use of severity maps (such as the US Forest Service's MTBS (Monitoring Trends in Burn Severity) and RAVG (Rapid Assessment of Vegetation Condition after Wildfire) programs, which can be used for post-fire restoration), the adoption of uncertainty-inclusive burn severity maps that come from independent, ecologically important metrics like those in our study can help inform management decisions by identifying areas of greater and lesser confidence in on-the-ground burn severity.

Our findings also highlight some limitations to the use of CBI and suggest some areas where additional information could increase its utility. Our analyses demonstrate that a plot-level value for CBI may not mean the same thing in different forests and incorporating information on pre-fire stand structure can help calibrate CBI to burn severity across fires. Information on stand density, QMD and tree height (variables that are not captured currently in the CBI protocol) could be helpful to know if CBI is likely to infer a greater than actual canopy burn severity. Where geographic information system (GIS) data are available for pre-fire forest structure in burned areas, maps of independent measures of burn severity could be adjusted based on the relationships between CBI and the independent measure given the stand structure context. This could help mitigate cases where the relationship between CBI and other measures varies substantially by pre-fire stand structure (e.g. Fig. 5*g*4). For example, in stands with tall trees (e.g. >35 m), large-diameter trees (e.g. QMD > 50) and high basal area (e.g. $>80\ m^2\ ha^{-1}$), a given value of CBI corresponds to lower values of canopy burn severity than stands with shorter, smaller-diameter trees and a lower total basal area. Finally, our study presents important information about conditions when CBI may be underpredicting burn severity, especially at the highest level of burn severity. In such conditions, CBI may fail to capture important fire effects such as deep char high in tree boles or high loss of biological legacies when consumption rates are high, factors that are important for post-fire forest recovery (Talucci and Krawchuk 2019; Turner *et al.* 2019). Additional field measurements to augment CBI (e.g. noting deep char or snag consumption) can help to capture extreme levels of burn severity where management action may need to respond with post-fire rehabilitation efforts.

Conclusion

In testing the relationship between CBI and independent burn severity metrics in co-located plots, we found that CBI captures most independent components of burn severity, and that these relationships can vary according to gradients of forest structure. Burn severity studies have relied on CBI to assess in-field burn severity since its development in 1996 (Morgan *et al.* 2014; Kolden *et al.* 2015), and our study suggests CBI has generally consistent relationships with independent field metrics. However, the relationship between CBI and some measures of burn severity varies across gradients of burn severity and forest structure. Our study builds further understanding of the relationship between CBI and independent field metrics and our models provide useful information for mapping ecologically meaningful fire effects. Potential modifications to CBI include collection of ancillary data such as the percentage of deep char in each vertical stratum, as well as redesigning CBI to have a scale that includes possibilities of the more extreme burn severity that has been observed in recent years. Testing and refining the methods for measuring burn severity are important in an era of increasing fire activity and changing fire regimes.

Data availability

Data are available on Zenodo: https://doi.org/10.5281/zenodo.5768751

Conflicts of interest

The authors declare no conflict of interest.

Declaration of funding

This project was funded by NSF Grant DEB-1719905 and USDA Agreement 17-CS-11130400–010 awarded to BJ Harvey. BJ Harvey acknowledges additional support from the University of Washington School of Environmental and Forest Sciences. SJ Saberi acknowledges financial support from the Graduation Opportunities and Minorities Achievement Program and the School of Environmental and Forest Sciences while completing her degree at the University of Washington.

Acknowledgements

We thank S. Salam, E. Pletcher, L. Walden, P. Hauschka, C. Zender and J. Weatherholt for help in the field. We thank EC Alvarado and DE Butman, MG Turner and JE Morris for insightful discussions and constructive feedback about this project, and MS Buonanduci for statistical advice. We thank C. Baker and the USDA Forest Service Geospatial Technology Applications Center (GTAC) for funding, logistical support and geospatial data. We thank M. Dillon and the University of Wyoming–National Park Service Research Station staff for logistical support and Yellowstone National Park, Grand Teton National Park, and the US Forest Service for facilitating this study under research permits specific to each field location.

References

Abatzoglou JT, Williams AP (2016) Impact of anthropogenic climate change on wildfire across western US forests. *Proceedings of the National Academy of Sciences of the United States of America* **113**, 11770–11775. doi:10.1073/PNAS.1607171113

Agee JK (1996) 'Fire Ecology of Pacific Northwest Forests.' (Island Press: Washington, DC)

Allen JL, Sorbel B (2008) Assessing the differenced Normalized Burn Ratio's ability to map burn severity in the boreal forest and tundra ecosystems of Alaska's national parks. *International Journal of Wildland Fire* **17**, 463–475. doi:10.1071/WF08034

Andrus RA, Veblen TT, Harvey BJ, Hart SJ (2016) Fire severity unaffected by spruce beetle outbreak in spruce-fir forests in southwestern Colorado. *Ecological Applications* **26**, 700–711. doi:10.1890/15-1121

Baker WL (2009) 'Fire ecology in Rocky Mountain landscapes.' (Island Press: Washington, DC)

Baldock JA, Smernik RJ (2002) Chemical composition and bioavailability of thermally altered *Pinus resinosa* (red pine) wood. *Organic Geochemistry* **33**, 1093–1109. doi:10.1016/S0146-6380(02)00062-1

Bird MI, Wynn JG, Saiz G, Wurster CM, McBeath A (2015) The Pyrogenic Carbon Cycle. *Annual Review of Earth and Planetary Sciences* **43**, 273–298. doi:10.1146/ANNUREV-EARTH-060614-105038

Bowman DMJS, Balch JK, Artaxo P, Bond WJ, Carlson JM, Cochrane MA, D'Antonio CM, DeFries RS, Doyle JC, Harrison SP, Johnston FH, Keeley JE, Krawchuk MA, Kull CA, Marston JB, Moritz MA, Prentice IC, Roos CI, Scott AC, Swetnam TW, van der Werf GR, Pyne SJ (2009) Fire in the Earth system. *Science* **324**, 481–484. doi:10.1126/SCIENCE.1163886

Brodie EG, Miller JED, Safford HD (2021) Productivity modifies the effects of fire severity on understory diversity. *Ecology* **102**, e03514. doi:10.1002/ECY.3514

Cansler CA, McKenzie D (2012) How robust are burn severity indices when applied in a new region? Evaluation of alternate field-based and remote-sensing methods. *Remote Sensing* **4**, 456–483. doi:10.3390/RS4020456

Cansler CA, McKenzie D (2014) Climate, fire size, and biophysical setting control fire severity and spatial pattern in the northern Cascade Range, USA. *Ecological Applications* **24**, 1037–1056. doi:10.1890/13-1077.1

Crookston NL, Dixon GE (2005) The forest vegetation simulator: a review of its structure, content, and applications. *Computers and Electronics in Agriculture* **49**, 60–80. doi:10.1016/J.COMPAG.2005.02.003

De Santis A, Chuvieco E (2009) GeoCBI: A modified version of the Composite Burn Index for the initial assessment of the short-term burn severity from remotely sensed data. *Remote Sensing of Environment* **113**, 554–562. doi:10.1016/J.RSE.2008.10.011

Dillon GK, Holden ZA, Morgan P, Crimmins MA, Heyerdahl EK, Luce CH (2011) Both topography and climate affected forest and woodland burn severity in two regions of the western US, 1984 to 2006. *Ecosphere* **2**, 130. doi:10.1890/ES11-00271.1

Donato DC, Campbell JL, Fontaine JB, Law BE (2009) Quantifying char in postfire woody detritus inventories. *Fire Ecology* **5**, 104–115. doi:10.4996/FIREECOLOGY.0502104

Dragozi E, Gitas IZ, Bajocco S, Stavrakoudis DG (2016) Exploring the relationship between burn severity field data and very high resolution GeoEye images: the case of the 2011 Evros wildfire in Greece. *Remote Sensing* **8**, 566. doi:10.3390/RS8070566

Dunn CJ, Bailey JD (2016) Tree mortality and structural change following mixed-severity fire in Pseudotsuga forests of Oregon's western Cascades, USA. *Forest Ecology and Management* **365**, 107–118. doi:10.1016/J.FORECO.2016.01.031

Eidenshink J, Schwind B, Brewer K, Zhu Z, Quayle B, Howard S (2007) A project for monitoring trends in burn severity. *Fire Ecology* **3**, 3–21. doi:10.4996/FIREECOLOGY.0301003

Furniss TJ, Kane VR, Larson AJ, Lutz JA (2020) Detecting tree mortality with Landsat-derived spectral indices: Improving ecological accuracy by examining uncertainty. *Remote Sensing of Environment* **237**, 111497. doi:10.1016/J.RSE.2019.111497

Harvey BJ, Donato DC, Romme WH, Turner MG (2013) Influence of recent bark beetle outbreak on fire severity and postfire tree regeneration in montane Douglas-fir forests. *Ecology* **94**, 2475–2486. doi:10.1890/13-0188.1

Harvey BJ, Donato DC, Turner MG (2014*a*) Recent mountain pine beetle outbreaks, wildfire severity, and postfire tree regeneration in the US Northern Rockies. *Proceedings of the National Academy of Sciences of the United States of America* **111**, 15120–15125. doi:10.1073/PNAS.1411346111

Harvey BJ, Donato DC, Romme WH, Turner MG (2014*b*) Fire severity and tree regeneration following bark beetle outbreaks: the role of outbreak stage and burning conditions. *Ecological Applications* **24**, 1608–1625. doi:10.1890/13-1851.1

Harvey BJ, Donato DC, Turner MG (2016) Burn me twice, shame on who? Interactions between successive forest fires across a temperate mountain region. *Ecology* **97**, 2272–2282. doi:10.1002/ECY.1439

Harvey BJ, Andrus RA, Anderson SC (2019) Incorporating biophysical gradients and uncertainty into burn severity maps in a temperate fire-prone forested region. *Ecosphere* **10**, e02600. doi:10.1002/ECS2.2600

Hood SM, Cluck DR, Smith SL, Ryan KC (2008) Using bark char codes to predict post-fire cambium mortality. *Fire Ecology* **4**, 57–73. doi:10.4996/FIREECOLOGY.0401057

Hudak AT, Morgan P, Bobbitt MJ, Smith AMS, Lewis SA, Lentile LB, Robichaud PR, Clark JT, McKinley RA (2007) The relationship of multispectral satellite imagery to immediate fire effects. *Fire Ecology* **3**, 64–90. doi:10.4996/FIREECOLOGY.0301064

Johnston JD, Dunn CJ, Vernon MJ (2019) Tree traits influence response to fire severity in the western Oregon Cascades, USA. *Forest Ecology and Management* **433**, 690–698. doi:10.1016/J.FORECO.2018.11.047

Johnstone JF, Allen CD, Franklin JF, Frelich LE, Harvey BJ, Higuera PE, Mack MC, Meentemeyer RK, Metz MR, Perry GL, Schoennagel T, Turner MG (2016) Changing disturbance regimes, ecological memory, and forest resilience. *Frontiers in Ecology and the Environment* **14**, 369–378. doi:10.1002/FEE.1311

Keeley JE (2009) Fire intensity, fire severity and burn severity: a brief review and suggested usage. *International Journal of Wildland Fire* **18**, 116–126. doi:10.1071/WF07049

Key CH, Benson NC (2006) Landscape assessment (LA) FIREMON: Fire effects monitoring and inventory system. USDA Forest Service, Rocky Mountain Research Station-General Technical Report 164-CD LA-1. (Ogden, UT)

Knipling EB (1970) Physical and physiological basis for the reflectance of visible and near-infrared radiation from vegetation. *Remote Sensing of Environment* **1**, 155–159. doi:10.1016/S0034-4257(70)80021-9

Kolden CA, Smith AMS, Abatzoglou JT (2015) Limitations and utilisation of Monitoring Trends in Burn Severity products for assessing wildfire severity in the USA. *International Journal of Wildland Fire* **24**, 1023–1028. doi:10.1071/WF15082

Korhonen L, Korhonen KT, Rautiainen M, Stenberg P (2006) Estimation of forest canopy cover: a comparison of field measurement techniques. *Silva Fennica* **40**, 577–588. http://jukuri.luke.fi/handle/10024/532615. doi:10.14214/SF.315

Miller JD, Thode AE (2007) Quantifying burn severity in a heterogeneous landscape with a relative version of the delta normalized burn ratio (dNBR). *Remote Sensing of Environment* **109**, 66–80. doi:10.1016/J.RSE.2006.12.006

Miller JD, Knapp EE, Key CH, Skinner CN, Isbell CJ, Creasy RM, Sherlock JW (2009) Calibration and validation of the relative differenced normalized burn ratio (RdNBR) to three measures of fire severity in the Sierra Nevada and Klamath Mountains, California, USA. *Remote Sensing of Environment* **113**, 645–656. doi:10.1016/J.RSE.2008.11.009

Morgan P, Keane RE, Dillon GK, Jain TB, Hudak AT, Karau EC, Sikkink PG, Holden ZA, Strand EK (2014) Challenges of assessing fire and burn severity using field measures, remote sensing and modelling. *International Journal of Wildland Fire* **23**, 1045–1060. doi:10.1071/WF13058

Ospina R, Ferrari SLP (2012) A general class of zero-or-one inflated beta regression models. *Computational Statistics & Data Analysis* **56**, 1609–1623. doi:10.1016/J.CSDA.2011.10.005

Parks SA, Holsinger LM, Koontz MJ, Collins L, Whitman E, Parisien M-A, Loehman RA, Barnes JL, Bourdon J-F, Boucher J, Boucher Y, Caprio AC, Collingwood A, Hall RJ, Park J, Saperstein LB, Smetanka C, Smith RJ, Soverel N (2019) Giving ecological meaning to satellite-derived fire severity metrics across North American forests. *Remote Sensing* **11**, 1735. doi:10.3390/RS11141735

Pausas JG (2015) Bark thickness and fire regime. *Functional Ecology* **29**, 315–327. doi:10.1111/1365-2435.12372

Pausas JG, Keeley JE (2021) Wildfires and global change. *Frontiers in Ecology and the Environment* **19**, 387–395. doi:10.1002/FEE.2359

Pearce J, Ferrier S (2000) Evaluating the predictive performance of habitat models developed using logistic regression. *Ecological Modelling* **133**, 225–245. doi:10.1016/S0304-3800(00)00322-7

Picotte JJ, Bhattarai K, Howard D, Lecker J, Epting J, Quayle B, Benson N, Nelson K (2020) Changes to the Monitoring Trends in Burn Severity program mapping production procedures and data products. *Fire Ecology* **16**, 16. doi:10.1186/S42408-020-00076-Y

R Core Team (2017) R: A language and environment for statistical computing. (R foundation for statistical computing: Vienna, Austria). Available at http://www.R-project.org/ [Verified 10 May 2021]

Ramsey F, Schafer D (2012) 'The Statistical Sleuth: A Course in Methods of Data Analysis, 3rd edn.' (Cengage Learning: Boston, MA).

Rigby RA, Stasinopoulos D (2005) Generalized additive models for location, scale and shape. *Journal of the Royal Statistical Society. Series C, Applied Statistics* **54**, 507–554. doi:10.1111/J.1467-9876.2005.00510.X

Soverel NO, Perrakis DDB, Coops NC (2010) Estimating burn severity from Landsat dNBR and RdNBR indices across western Canada. *Remote Sensing of Environment* **114**, 1896–1909. doi:10.1016/J.RSE.2010.03.013

Soverel NO, Coops NC, Perrakis DDB, Daniels LD, Gergel SE (2011) The transferability of a dNBR-derived model to predict burn severity across 10 wildland fires in western Canada. *International Journal of Wildland Fire* **20**, 518–531. doi:10.1071/WF10081

Stenzel JE, Bartowitz KJ, Hartman MD, Lutz JA, Kolden KA, Smith AMS, Law BE, Swanson ME, Larson AJ, Parton WJ, Hudiburg TW (2019) Fixing a snag in carbon emissions estimates from wildfires. *Global Change Biology* **25**, 3985–3994. doi:10.1111/GCB.14716

Stevens JT, Kling MM, Schwilk DW, Varner JM, Kane JM (2020) Biogeography of fire regimes in western U.S. conifer forests: A trait-based approach. *Global Ecology and Biogeography* **29**, 944–955. doi:10.1111/GEB.13079

Talucci AC, Krawchuk MA (2019) Dead forests burning: the influence of beetle outbreaks on fire severity and legacy structure in sub-boreal forests. *Ecosphere* **10**, e02744. doi:10.1002/ECS2.2744

Turner MG, Braziunas KH, Hansen WD, Harvey BJ (2019) Short-interval severe fire erodes the resilience of subalpine lodgepole pine forests. *Proceedings of the National Academy of Sciences of the United States of America* **116**, 11319–11328. doi:10.1073/PNAS.1902841116

Westerling AL (2016) Increasing western US forest wildfire activity: sensitivity to changes in the timing of spring. *Philosophical Transactions of the Royal Society of London. Series B, Biological Sciences* **371**, 20150178. doi:10.1098/RSTB.2015.0178

Whitman E, Parisien M-A, Thompson DK, Hall RJ, Skakun RS, Flannigan MD (2018) Variability and drivers of burn severity in the northwestern Canadian boreal forest. *Ecosphere* **9**, e02128. doi:10.1002/ECS2.2128